Available online at www.sciencedirect.com

SciVerse ScienceDirect

00 (2014) 000–000

Procedia Computer Science

Fourth International Conference on Selected Topics in Mobile & Wireless Networking (MoWNet'2014)

Network coded MIMO aided cooperative communications in the ambulance-and-emergency area

Hung Viet Nguyen[a,*], Zunaira Babar[a], Soon Xin Ng[a], Matteo Mazzotti[b], Lorenzo Iacobelli[c], and Lajos Hanzo[a]

[a]*School of Electronics and Computer Science, University of Southampton, SO17 1BJ, United Kingdom*
[b]*Consorzio Nazionale Interuniversitario Per Le Telecomunicazioni, Via Venezia 52, 47521 Cesena (FC), Italy*
[c]*Thales Communications and Security, SAS 4, avenue des Louvresses, 92622 Gennevilliers Cedex, France*

Abstract

In this contribution, a novel network coding (NC) aided multi-input multi-output (MIMO) scheme is proposed for providing reliable transmission from an ambulance assisting in an emergency situation by cooperating with relaying devices at an emergency scene. Our system is constituted by an Irregular Convolutional Coded Unity Rate Coded Space Time Trellis Coded M-ary Phase Shift Keying (IrCC-URC-STTC-MPSK) scheme invoked for exploiting the benefits of MIMO systems. The system is designed with the aid of Extrinsic Information Transfer (EXIT) charts for approaching the corresponding channel capacity in fast fading environments. The proposed scheme exhibits substantial benefits over conventional MIMO systems in hostile wireless channels.

Peer-review under responsibility of organizing committee of Fourth International Conference on Selected Topics in Mobile & Wireless Networking (MoWNet'2014).

Keywords: emergency area; cooperative communications; network coding.

1. Introduction

The ultimate aim of designing a wireless communication system is to provide reliable high data rate links, which can be improved by utilising various types of diversity techniques, e.g. spatial-diversity, temporal-diversity and frequency-diversity. The so-called cooperative diversity, a form of spatial diversity, has been introduced in[1] in order to create a Virtual Antenna Array (VAA) with the aid of cooperating single-antenna-aided mobiles for providing independent fading transmission paths.

Space Time Trellis Codes (STTCs)[2] and Space Time Block Codes (STBCs)[3], which are joint coding and transmit-receive diversity aided MIMO systems, constitute efficient techniques of communicating over fading channels[4]. We note, however that STTCs are capable of attaining coding gain in addition to their spatial diversity gain, while the STBCs of [5] can only achieve a spatial diversity gain[6] but no coding gain. Additionally, Tüchler and Hagenauer[7] proposed the employment of IRregular Convolutional Codes (IRCCs) for serially concatenated schemes,

* Hung Viet Nguyen
E-mail address: hvn08r@ecs.soton.ac.uk

Peer-review under responsibility of organizing committee of Fourth International Conference on Selected Topics in Mobile & Wireless Networking (MoWNet'2014).

which are constituted by a family of convolutional codes having different rates, in order to design a near-capacity system. As demonstrated in[8], IrCC-URC-STTC coding arrangement is capable of approaching the Discrete-input Continuous-output Memoryless Channel (DCMC) capacity of the MIMO systems.

As the epitome of collaboration, network coding is a recently introduced paradigm[9] conceived for efficiently disseminating data in multicast wireless networks, where the data flows arriving from multiple sources are combined to achieve compression and hence to increase the achievable throughput[10]. Network codes may be classified based on different perspectives. For example on the basis of how the information streams are processed at the relays[11], or depending on the construction of network codes[12], depending on the specific the architecture of networks employing network coding[13], the layer in networks where the network coding operates[14], just to name a few. Three well-known categories of network codes are Linear Network Codes (LNC), Non-linear Network Codes (NLNC) and the family of so-called Hybrid Network Codes (HNC). It is suggested by[15,16] that LNC has many attractive properties. From a theoretical standpoint, linearity is a beneficial algebraic property supported by exact mathematical foundations. From an engineering standpoint, the simplicity of linear approaches leads to relatively low complexity in the encoding and decoding processes. In LNC systems, the relay nodes store the incoming packets in their own buffer and then transmit the linear combinations of these packets. The coefficients used for creating the linear combination may be random numbers defined over a large finite field[17,18], or those gleaned from parity-check matrices of error control codes[19,20].

Generalised Dynamic Network Codes (GDNC) constitute an extension of the Dynamic Network Codes (DNC) recently proposed in[21]. Further designs were provided in [20,22] by considering the problem as being equivalent to that of designing linear block codes defined over Galois Field GF(q) for erasure correction. In [20,22], the authors investigated the GDNC system assuming an idealised or so-called 'perfect' channel coding scheme, which was defined as the code that is capable of operating at the Continuous-input Continuous-output Memoryless Channel's (CCMC) capacity. Some of recent work has extended the network coding scheme to the scenario of employing realistic Single-Input Single-Ouput (SISO) channel coding schemes[23,24].

Against this background, novel network coding aided MIMO schemes are designed for combatting the deleterious effects of both the shadow fading and of the Rayleigh fading in hostile wireless channels. More specifically, a powerful IrCC-URC-STTC is proposed for providing a near-capacity performance in fast fading environments. Additionally, network coding is invoked for collaboration in order to equip the system with a further space diversity gain for combatting slow fading effects imposed by obstacles blocking the transmission links spanning from the ambulance's transmitter to the base station, where heterogeneous data to/from an ambulance in an emergency situation are transmitted. Accordingly, both diagnostic data (e.g. live ultrasound videos) and other types of information (e.g. ambient videos) have to be transmitted to the hospital while the ambulance is stationary or on the move. The availability of the information may allow remote specialists to pre-arrange the hospitalisation for the patients and/or to guide local staff during first-aid operations. In this context, it becomes crucially important to guarantee a throughput sufficiently high to support single or multiple video transmissions associated with a low outage probability. In this regard, the proposed schemes may help to improve the reliability of the end-to-end link, in order to facilitate the quality of experience (QoE) of the final users, namely doctors and specialists. The rest of this paper is organised as follows.

In Section 2, our proposed system model is portrayed, before providing details of our design principles as well as design examples for the general IrCC-URC-STTC scheme. The network coding applied in our system is analysed in Sec. 3.3. Finally, in Section 4, we present our simulation results and associated discussions, before offering our conclusions.

2. System Model

In this paper, we consider a network coding aided multi-input multi-output (NC-MIMO) based system supporting a USER (an ambulance) communicating with a BS, where other relaying devices (RELAY) operating in the vicinity of the emergency scene can support the USER-BS transmissions by cooperating with the aid of network coding. As portrayed in Fig. 1 exemplifying our system, a transmission session is conducted in two groups of phases, the broadcast phases and the cooperative phases. During the broadcast phases, the USER broadcasts $k_1 = 2$ information frames, namely I_1, I_2, where I_i seen in Fig. 1 represents an information frame (packet or message) transmitted by the USER. This operation takes place during the specific broadcast phase i selected from the entire set of k_1 broadcast phases. Then, during the cooperative phases, each relaying device transmits $k_2 = 1$ parity frames, namely $\boxplus P_1(1), P_2(2)$, containing nonbinary linear combinations of the information frames that were successfully received at the RELAY. The

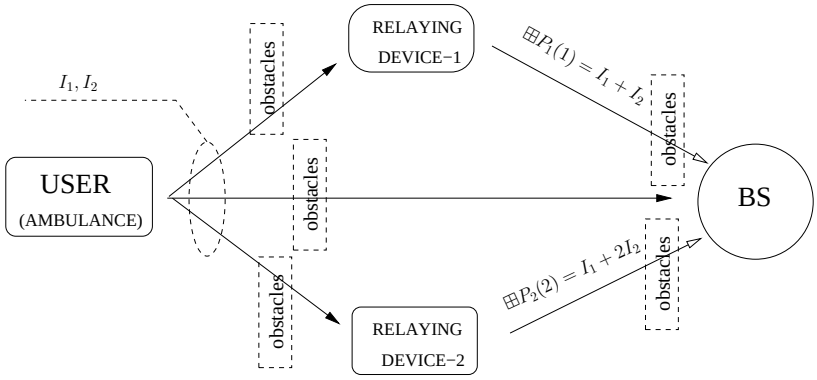

Figure 1: The model of the NC-aided MIMO system, where the USER transmits two information frames, namely I_1 and I_2 in two broadcast phases and each RELAY transmits a parity frame of $P_1(1)$ (or $P_2(2)$) during two cooperative phases.

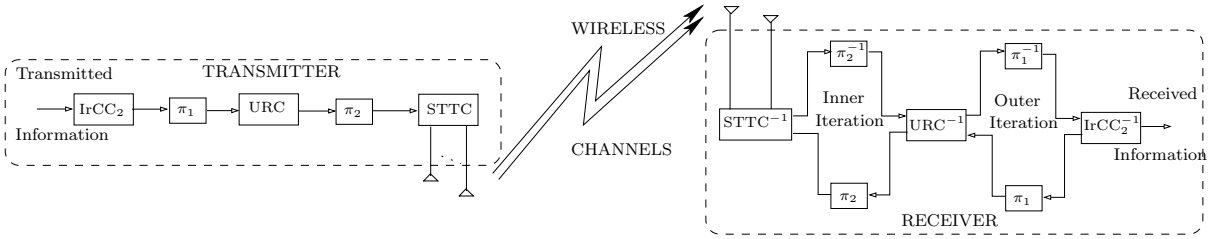

Figure 2: The structure of the Irregular Convolutional Coded Unity Rate Coded Space Time Trellis Code (IrCC-URC-STTC) coding scheme.

notation $\boxplus P_p(t)$ in Fig. 1 represents the parity frame transmitted by the RELAY p during the cooperative phase t, and $\boxplus$ represents a specific nonbinary linear combination, where the weighting coefficients are defined by the systematic generator matrix G of Reed Solomon (RS) codes defined over the GF(q).

Note that a single phase is defined as a time period, in which a user performs a single transmission over the appropriately created orthogonal channels either in the time-, frequency- or code- domain. For the sake of simplicity, the channels are deemed to be orthogonal in the time domain.

Our system may be viewed being constructed by two layers, where the first layer represents the point-to-point transmission links, namely between USER and BS, USER and RELAY, or RELAY and BS employing the IrCC-URC-STTC coding scheme, as detailed in Sec. 2.1. The second layer represents the cooperative actions carried out by the USER, the BS and the RELAY as modelled by the example provided in Sec. 1.

2.1. IrCC-URC-STTC coding scheme

In the IrCC-URC-STTC scheme pictured in Fig. 2, the bit stream at the transmitter side is first encoded by the IrCC encoder, then interleaved by the interleaver π_1, in order to get the interleaved input stream of the URC encoder. The output of the URC encoder is again scrambled by the interleaver π_2 before being encoded by the STTC. This signal is then transmitted to the receiver side over wireless fading channels, as portrayed in Fig. 2 .

At the receiver side, as seen in Fig. 2, the signals received from antenna are demodulated and decoded by the STTC decoder before being processed in the I inner iterations exchanging extrinsic information between the STTC decoder and the URC decoder. The resultant soft information extracted from the received signals by the inner iterations are then used as the input data for the J outer iterations exchanging extrinsic information between the IrCC encoder and the amalgamated inner component, which is the Unity Rate Coded M-ary Phase Shift Keying (URC-STTC-MPSK) arrangement.

2.2. Network-Coding layer

In the network coding layer of our system, information frames are combined at the relaying devices for the sake of providing our system with additional space diversity. Let us illustrate the transmission session of the system by a transfer matrix as

$$\boldsymbol{G}_{2\times4} = \left[\begin{array}{cc|cc} 1 & 0 & 1 & 1 \\ 0 & 1 & 1 & 2 \end{array}\right], \tag{1}$$

where $\boldsymbol{G}_{2\times4}(1,1)$ and $\boldsymbol{G}_{2\times4}(2,2)$ represent the success/failure of the transmission of information frame I_1 and I_2 from the USER to the BS, while the parity frame transmitted by RELAY-1 (RELAY-2) during the cooperative phase C_1 (or C_2) is given by $P_1(1) = \boldsymbol{G}_{2\times4}(1,3)I_1 + \boldsymbol{G}_{2\times4}(2,3)I_2$ (or $P_2(2) = \boldsymbol{G}_{2\times4}(1,4)I_1 + \boldsymbol{G}_{2\times4}(2,4)I_2$).

Let us define $\boldsymbol{G}'_{2\times4}$ as the corresponding *modified* transfer matrix, where the terminology *modified* implies that the entries of $\boldsymbol{G}'_{2\times4}$ are modified with respect to those of the original transfer matrix $\boldsymbol{G}_{2\times4}$ of (1) in order to reflect the success/failure of each transmission within a transmission session. If all the frames transmitted within the session are successfully decoded, the transmission session can be equivalently represented by the modified transfer matrix $\boldsymbol{G}'_{2\times4} = \boldsymbol{G}_{2\times4}$.

In order to demonstrate how the modified matrix may be determined, let us consider the following example of the actual transmission session, where $'\xrightarrow{I_i}'$ represents the transmission direction of the information frame I_i, while $' = 1'$ (or $' = 0'$) above the arrows indicates that the frame was successfully (or unsuccessfully) recovered at the destination:

$$B_1: \ [\text{USER} \xrightarrow{I_1,=1} \text{BS}] : \boldsymbol{G}'_{2\times4}(1,1) = \boldsymbol{G}_{2\times4}(1,1), \tag{2}$$

$$[\text{USER} \xrightarrow{I_1,=1} \text{RELAY-1}] : \boldsymbol{G}'_{2\times4}(1,3) = \boldsymbol{G}_{2\times4}(1,3), \tag{3}$$

$$[\text{USER} \xrightarrow{I_1,=0} \text{RELAY-2}] : \boldsymbol{G}'_{2\times4}(1,4) = 0; \tag{4}$$

$$B_2: \ [\text{USER} \xrightarrow{I_2,=0} \text{BS}] : \boldsymbol{G}'_{2\times4}(2,2) = 0, \tag{5}$$

$$[\text{USER} \xrightarrow{I_2,=0} \text{RELAY-1}] : \boldsymbol{G}'_{2\times4}(2,3) = 0, \tag{6}$$

$$[\text{USER} \xrightarrow{I_2,=1} \text{RELAY-2}] : \boldsymbol{G}'_{2\times4}(2,4) = \boldsymbol{G}_{2\times4}(2,4), \tag{7}$$

$$C_1: \ [\text{RELAY-1} \xrightarrow{P_1(1),=1} BS] : \boldsymbol{G}'_{2\times4}(i,3) = \text{unchanged}, i = 1,2; \tag{8}$$

$$C_2: \ [\text{RELAY-2} \xrightarrow{P_2(2),=0} BS] : \boldsymbol{G}'_{2\times4}(i,4) = 0, i = 1,2. \tag{9}$$

Given the transmission links described by (2)-(9), the transmission session can be represented by the modified matrix of $\boldsymbol{G}'_{2\times4}$ formulated as:

$$\boldsymbol{G}'_{2\times4} = \left[\begin{array}{cc|cc} 1 & 0 & 1 & 0 \\ 0 & 0 & 0 & 0 \end{array}\right], \tag{10}$$

where the $\boldsymbol{G}'_{2\times4}(2,2)$ in (10) becomes "0" owing to the unsuccessful [USER $\xrightarrow{I_2,=0}$ BS] transmission of the information frame I_2 during the broadcast phase B_2, as represented by (5). The "0" elements in the fourth column of (10) indicate the unsuccessful [RELAY-2 $\xrightarrow{P_2(2),=0}$ BS] transmission during the cooperative phase C_2, as portrayed by (9). Since the transmission [RELAY-1 $\xrightarrow{P_1(1),=1}$ BS] of the parity frame $P_1(1)$ is successfully concluded, the value "0" in column 3 of the modified matrix of (10) represents the failure of the transmission [USER $\xrightarrow{I_2,=0}$ RELAY-1] in the broadcast phase B_1, as detailed by (6).

In order to efficiently detect the information frames, the BS has to be aware of how each parity frame was constructed at the RELAYs. In line with[21] we assume that this information is available, noting that naturally the related side-information imposes an additional overhead. Fortunately, this side-information may be deemed negligible, when sufficiently long information frames are used.

3. Designs and Analysis

In this section, the design and performance analysis of the first layer is presented in Sec. 3.1 and in Sec. 3.2, respectively. Our IrCC-URC-STTC aided network coding scheme is further discussed in Sec. 3.3.

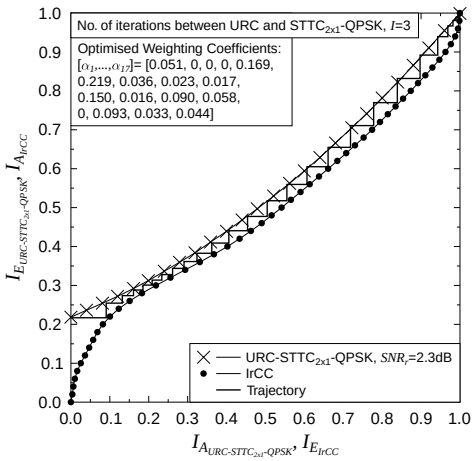

Figure 3: The EXIT chart curves of the URC-STTC-QPSK having two transmit and one receive antennas (URC-STTC$_{2\times1}$-QPSK) scheme at $SNR = 2.3$ dB when $I = 3$ iterations between URC and STTC$_{2\times1}$-QPSK are configured and of the IrCC having the overall coding rate $R_c = 0.5$.

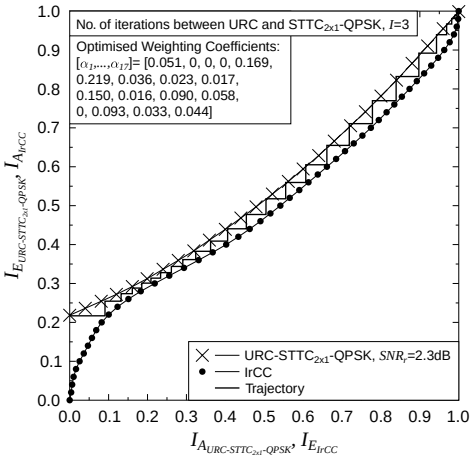

Figure 4: Achievable throughputs of the MIMO$_{2\times1}$-QPSK, the STTC$_{2\times1}$-QPSK arrangement, the URC-STTC$_{2\times1}$-QPSK arrangement ($I = 0, 3$ iterations between URC and URC-STTC$_{2\times1}$-QPSK) and the IrCC-URC-STTC$_{2\times1}$-QPSK arrangement ($I = 3$ iterations between URC and URC-STTC$_{2\times1}$-QPSK in conjunction with $J = 24$ iterations between IrCC and URC-STTC$_{2\times1}$-QPSK).

3.1. EXIT-chart matching and optimisation of the IrCC-URC-STTC-MPSK scheme

This section is dedicated to the design of our first coding layer employing the IrCC-URC-STTC-MPSK coding arrangement portrayed in Fig. 2 and detailed in Sec. 2.1.

Firstly, we design the two stage inner arrangement URC-STTC-QPSK. Secondly, the code design is continued by viewing our three-stage IrCC-URC-STTC-QPSK coding arrangement as the two-stage-concatenated IrCC outer code and the amalgamated URC-STTC-QPSK inner code. The details of our design using the EXIT chart matching procedure conceived for this coding arrangement is briefly summarised as follows:

Step1.1: In order to increase the achievable channel capacity of the amalgamated URC-STTC-QPSK inner code and to approach that of a STTC and STTC-QPSK aided system, an iterative decoding process exchanging extrinsic information between the URC and STTC decoders should be implemented[25]. We exploit the above-mentioned characteristics of EXIT charts[26] for calculating the DCMC capacity of the two inner-most coding arrangements, namely that of the STTC-QPSK and URC-STTC-QPSK schemes. Then, based on the capacity of these two coding arrangements, we determine the most appropriate number of iterations. As a result, Fig. 4 shows that once at least $I = 3$ iterations had been applied, the achievable channel capacities of the STTC-QPSK and URC-STTC-QPSK systems become near-identical.

Step1.2: Create the EXIT chart of the URC-STTC-QPSK scheme for different receiver Signal to Noise Ratios SNR_r, as seen in Fig. 3.

Step2: Fix the overall IrCC code rate to $R_c = 0.5$ and employ the EXIT curve matching algorithm [7] for generating the optimised weighting coefficients $\alpha_j, j = 1, ..., 17$, of the 17-subcode IrCC codes corresponding to the lowest possible SNR_r that allows decoding convergence, where the decoding trajectory reaches the top-right corner of the corresponding EXIT charts. This observation suggests that a near-capacity performance can be achieved.

Once the steps mentioned above have been completed, we obtain the EXIT curves and the corresponding weighting coefficients α_j, $j = 1, ..., 17$ for the IrCC encoder, as shown in Fig. 3. The EXIT-chart results show that if having $J = 24$ iterations were affordable, the iterative decoding trajectory would reach the $(1, 1)$ point of perfect convergence to an infinitesimally low BER.

Again, by exploiting the area property of the EXIT-charts[27,26], the achievable DCMC capacities of the MIMO$_{2\times1}$-QPSK, the STTC$_{2\times1}$-QPSK, URC-STTC$_{2\times1}$-QPSK and IrCC-URC-STTC$_{2\times1}$-QPSK aided systems are quantified by

generating the EXIT charts of these schemes across various SNR values. Then, the areas under each of these EXIT charts corresponding to different SNR values are measured for determining the associated capacity curves, as plotted in Fig. 4.

It should be noted that the capacity of an inner arrangement sets an upper bound for the capacity of an outer arrangement. Hence, according to the afore-listed order, the capacity associated with the inner most arrangement $MIMO_{2\times1}$-QPSK sets the maximum achievable capacity for all the systems employing the other schemes, namely the $STTC_{2\times1}$-QPSK, URC-$STTC_{2\times1}$-QPSK and IrCC-URC-$STTC_{2\times1}$-QPSK, as seen in Fig. 4. Additionally, it can be seen from Fig. 3 and Fig. 4 that the IrCC-URC-STTC-QPSK scheme's capacity curve is only about $(2.3 - 1.6) = 0.7$dB away from the STTC-based DCMC capacity curve.

Following the same procedure as illustrated by designing the IrCC-URC-STTC-QPSK, we also designed other coding arrangements relying on 8PSK and 16PSK, namely the IrCC-URC-STTC-8PSK and IrCC-URC-STTC-16PSK schemes. The corresponding weighting coefficients of the IrCC encoder are listed in Table 1.

Table 1: Subcode weighting coefficients of the IrCC encoder associated with URC-STTC-QPSK, URC-STTC-8PSK and URC-STTC-16PSK.

Arrangement (Turbo-cliff SNR **)**	**Coefficients:** $[\alpha_1, \alpha_2, ..., \alpha_{17}]$
URC-STTC-QPSK (2.3 dB)	[0.05, 0, 0, 0 0.169, 0.219, 0.036, 0.023, 0.0166, 0.149, 0.015, 0.089, 0.058, 0, 0.093, 0.033, 0.044]
URC-STTC-8PSK (4.4 dB)	[0 0.171, 0.093, 0, 0, 0.195, 0, 0, 0.099, 0.05, 0, 0, 0.197, 0, 0, 0.025, 0.165]
URC-STTC-16PSK (7.0 dB)	[0.203, 0, 0.093, 0 0.102, 0, 0, 0.148, 0, 0, 0 0.055, 0.149, 0, 0, 0, 0.248]

3.2. Performance of IrCC-URC-STTC-MPSK coding scheme

Upon employing the IrCC weighting coefficients listed in Tab. 1, we can now evaluate the BER-performance of our coding schemes, namely of both our IrCC-URC-STTC-QPSK and IrCC-URC-STTC-16PSK schemes, which rely on different modulation arrangements, such as QPSK and 16PSK, as shown in Fig. 5. For the sake of clarity, it should be noted that we only present the results associated with QPSK and 16PSK in Fig. 5 and Fig. 6. Observe in Fig. 5 that our Monte-Carlo simulation results substantiate the predictions obtained by using the EXIT-charts of Fig. 3, as we illustrated earlier in Section 3.1 by using the example of the IrCC-URC-STTC-QPSK coding scheme. For the scenarios of employing 8PSK and 16PSK, the IrCC coefficients and the corresponding 'turbo-cliff' SNRs facilitating a vanishingly low BER are summarised in Table 1, which were obtained by our EXIT-chart based design.

Importantly, the value of the 'turbo-cliff' SNR given in Table 1 indicates that as we inferred from our EXIT-chart analysis upon Fig. 3, once the SNR value exceeds this value, the BER/FER of the coding scheme is expected to become infinitesimally low. Indeed, the performance prediction provided by the EXIT-chart curves of Fig. 3 is fulfilled by our simulation results presented in Fig. 5. Explicitly, the BER of the system supported by our coding schemes, such as the IrCC-URC-STTC-QPSK, IrCC-URC-STTC-8PSK and IrCC-URC-STTC-16PSK arrangements, drops to a value below 10^{-6}, when the SNR value exceeds the corresponding turbo-cliff SNR.

However, as suggested in [28], in the small-scale fading channel, the transmitter can send data at the rate of $R < C|_h$, while maintaining an arbitrarily low error probability. By contrast, this idealised performance cannot be maintained for large-scale fading channels. This phenomenon is also confirmed by the performance of our system employing merely the first MIMO layer in the presence of the large-scale (slow) fading, as seen in Fig. 5. As a result of the detrimental influence associated with the slow fading, our system performance degraded by about 45 dB at an $FER = 10^{-4}$, as seen in Fig. 5. Hence, the network coding layer is then invoked for eliminating or mitigating this performance degradation.

3.3. Diversity order and relay position

As suggested in [20,22], the diversity order reflecting the degree of space diversity gain attained by employing network coding may be presented in our scenario as

$$D_{NC} = N_r + k_2 \ . \tag{11}$$

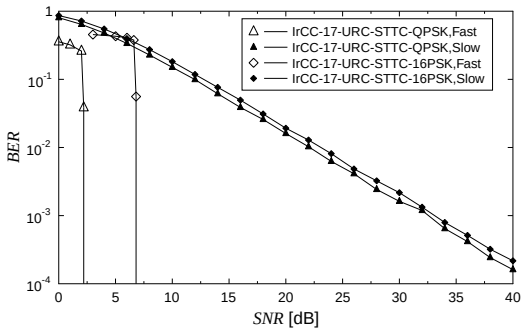

Figure 5: BER performance of IrCC-URC-STTC$_{2\times1}$-MPSK corresponding to different modulation schemes, namely QPSK and 16PSK over Rayleigh small-scale (fast) and large-scale (slow) fading channels, where the coding rate $R_c = 0.5$ and the frame length $N = 10^5$ are employed, while the weighting coefficients of the IrCC are given in Tab. 1.

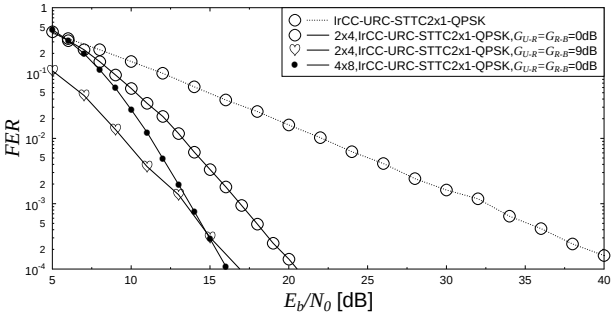

Figure 6: FER performance of the proposed NC-aided-MIMO systems associated with the $G_{2\times4}$ and $G_{4\times8}$ network coding codec, where IrCC-URC-STTC$_{2\times1}$-QPSK are deployed, while two RELAYs at the position pertaining to a minimum RDRPLR gain of $G_{U-R} = G_{R-B} = 0$dB (or to a maximum RDRPLR gain $G_{U-R} = G_{R-B} = 9$dB) are activated.

where the number of relays N_r is assumed to be the same value as the number of users in context of the system proposed in [20,22]. Let us focus our attention on the network coding rate R_{NC} characterising the multiplexing capability of the network coding layer exemplified in Sec. 2.2, which may be expressed as

$$R_{NC} = \frac{\text{Total number of information frames}}{\text{Total number of transmitted frames}} = \frac{k_1}{k_1+N_r k_2} \ . \tag{12}$$

By further considering Equations (11) and (12), it can be inferred that we may conceive different systems having the same rate R_{NC} but different diversity order D_{NC} which is achieved by independently adjusting k_1, k_2 and N_r. The matrix $\boldsymbol{G}_{4\times8}$ [29]:

$$\boldsymbol{G}_{4\times8} = \left[\begin{array}{cccc|cccc} 1&0&0&0&3&7&3&6 \\ 0&1&0&0&5&7&7&4 \\ 0&0&1&0&2&4&6&1 \\ 0&0&0&1&5&5&3&2 \end{array}\right] \tag{13}$$

defined over GF(8) constitutes a beneficial candidate matrix for constructing $\boldsymbol{G}_{4\times8}$-based system. The system is expected to be capable of providing an improved FER performance in comparison to that of the $\boldsymbol{G}_{2\times4}$-based one.

In contrast to the model investigated in [20,22,24], where the users are also act as relays and where the lengths of all the links in the system were assumed to be equal, in our system we consider RELAYs located at diverse positions. Accordingly, if we use the path-loss between USER and BS as a reference, the reduced-distance-related pathloss reduction (RDRPLR) gain for the USER-RELAY link achieved by having a RELAY located at a distance of d_{U-R} is given by [30,31]:

$$g_{U-R} = \left(\frac{d_{U-R}}{d_{U-B}}\right)^{\alpha} \ , \tag{14}$$

where α is the path-loss exponent [32]. Similarly, the RDRPLR gain for the RELAY-BS link with respect to the USER-BS link is given by:

$$g_{R-B} = \left(\frac{d_{R-B}}{d_{U-B}}\right)^{\alpha} \ . \tag{15}$$

For the sake of brevity, we only characterise the performance of our system associated with the RELAYs located at an equal distance from the USER and BS. For exploiting the advantageous position of the RELAYs, the system only exploits the RELAYs satisfying both $d_{U-R} \leq d_{U-B}$ and $d_{R-B} \leq d_{U-B}$. Accordingly, considering the path-loss exponents of $\alpha = 1, 2, 3$, the RDRPLR ranges from $G_{U-R} = G_{R-B} = 0$dB to $G_{U-R} = G_{R-B} = 9$dB.

4. Simulation Results and Discussions

In this section, we will provide simulation and numerical results for quantifying the benefits of our proposed system in combatting both slow fading and fast fading. For the sake of simplicity, we used the above-mentioned $\boldsymbol{G}_{2\times4}$ and $\boldsymbol{G}_{4\times8}$ based systems as examples.

It should be noted that the performance of our system in Fig. 5 is presented in the form of FER-versus-SNR curves, for facilitating the comparison of the performance results in Fig. 5 and corresponding results gleaned by EXIT chart analyses, as presented in Tab. 1. By contrast, the performance presented in Fig. 6 is formulated in the form of FER-versus-E_b/N_0 for highlighting a fair comparison between the different system configurations pertaining to distinct aggregate coding rates.

Let us now recall our results presented in Fig. 5, where our system performance was shown to be degraded approximately 45 dB at an FER of 10^{-4}, when the effects of the slow fading is taken into consideration, in addition to those of the fast fading. As mentioned in Sec. 2.2 and in Sec. 2.2, the proposed network coding layer may be able to assist our system in combating the grave influence of slow fading. As demonstrated in Fig. 6, the degradation imposed was compensated by employing the network coding aided cooperation in our system. Accordingly, the slow-fading-induced degradation is reduced by 26 dB and 22 dB, when the network coding codec relied on $\boldsymbol{G}_{2\times4}$ and on $\boldsymbol{G}_{4\times8}$, respectively, while the IrCC-URC-STTC$_{2\times1}$-QPSK scheme was activated in the channel coding layer of our system.

The significant reduction in the system's performance degradation achieved by employing the network coding aided cooperation raises the deep-rooted question as to that how the network coding succeeds in compensating the degradation imposed by slow fading channels. Recall from Equations (11) and (12) that the second layer characterising the network coding operation can be configured for having the same information rate but offering different diversity orders. Accordingly, we expect that a better performance is confirmed for the system associated with the higher diversity order of $\boldsymbol{G}_{4\times8}$. As seen in Fig. 6, the system's performance improvement becomes approximately 4 dB at an $FER = 10^{-4}$ by activating the $\boldsymbol{G}_{4\times8}$ configuration over that of $\boldsymbol{G}_{2\times4}$ associated configuration, provided that the IrCC-URC-STTC$_{2\times1}$-QPSK scheme is employed in the first MIMO layer of our system. However, the design of the optimum network coding layer remains an open problem. As another open issue, the advantageous position of the RELAYs is capable of providing a significant system's improvement, namely of approximately 4dB at an $FER = 10^{-4}$, as seen in Fig. 6.

5. Conclusions

In this contribution, we proposed the network coding aided multi-input multi-output systems for our IRCC-URC-STTC$_{2\times1}$-MPSK scheme invoked by the USER, RELAYs and BS. Network coding was invoked for cooperative communications amongst the USER, RELAYs and BS. Our proposed NC-aided-MIMO system provided a significant performance improvement of at least 22 dB at an FER of 10^{-4}, compared to the corresponding conventional MIMO system. The improvement may help to guarantee a throughput sufficiently high to support single or multiple video transmissions along with a low outage probability in order to facilitate the quality of experience (QoE) of the final users, namely doctors and specialists, in the context of heterogeneous data transmissions required in ambulance-and-emergency areas.

Acknowledgements

The financial support of the European Research Council's Advanced Fellow Grant, that of the India-UK Advanced Technology Centre, as well as that of the European Union's Seventh Framework Programme (FP7/2007-2013) under the auspices of the CONCERTO project (grant agreement no 288502) is gratefully acknowledged.

References

1. J. Laneman, G. Wornell, Distributed space-time-coded protocols for exploiting cooperative diversity in wireless networks, IEEE Transactions on Information Theory 49 (10) (2003) 2415 – 2425. doi:10.1109/TIT.2003.817829.

2. V. Tarokh, N. Seshadri, A. R. Calderbank, Space-time codes for high data rate wireless communication: performance criterion and code construction, IEEE Transactions on Information Theory 44 (2) (1998) 744–765. doi:10.1109/18.661517.
3. S. M. Alamouti, A simple transmit diversity technique for wireless communications, IEEE Journal on Selected Areas in Communications 16 (8) (1998) 1451–1458. doi:10.1109/49.730453.
4. V. Tarokh, A. Naguib, N. Seshadri, A. R. Calderbank, Space-time codes for high data rate wireless communication: performance criteria in the presence of channel estimation errors, mobility, and multiple paths, IEEE Transactions on Communications 47 (2) (1999) 199–207. doi:10.1109/26.752125.
5. S. X. Ng, S. Das, J. Wang, L. Hanzo, Near-capacity iteratively decoded space-time block coding, in: Proc. IEEE Vehicular Technology Conference VTC Spring 2008, 2008, pp. 590–594. doi:10.1109/VETECS.2008.132.
6. L. Hanzo, O.Alamri, M. E.Hajjar and N.Wu, Near-Capacity Muti-Functional MIMO Systems, John Wiley and Sons, New York, USA , 2009.
7. M.Tücher, J. Hagenauer, Exit charts of irregular codes, in: Proceeding of the 36th Annual Conference on Information Sciences and Systems [CDROM], (Princeton, NJ, USA), 2002. doi:10.1109/VETECF.2004.1400303.
8. H. V. Nguyen, S. X. Ng, L. Hanzo, Distributed three-stage concatenated irregular convolutional, unity-rate and space-time trellis coding for single-antenna aided cooperative communications, in: Vehicular Technology Conference Fall (VTC 2010-Fall), 2010 IEEE 72nd, 2010, pp. 1–5. doi:10.1109/VETECF.2010.5594321.
9. R. Ahlswede, N. Cai, S.-Y. Li, R. Yeung, Network information flow, IEEE Transactions on Information Theory 46 (4) (2000) 1204 –1216. doi:10.1109/18.850663.
10. A. Asterjadhi, E. Fasolo, M. Rossi, J. Widmer, M. Zorzi, Toward network coding-based protocols for data broadcasting in wireless ad hoc networks, IEEE Transactions on Wireless Communications 9 (2) (2010) 662 –673. doi:10.1109/TWC.2010.02.081057.
11. C. Fragouli, E. Soljanin, Network coding fundamentals, Foundation and Trends in Networking 2 (1) (2007) 1–133. doi:10.1561/1300000003.
12. Z. Zhang, Theory and applications of network error correction coding, Proceedings of the IEEE 99 (3) (2011) 406 –420. doi:10.1109/JPROC.2010.2093551.
13. Y. R.W., C. N. Li S.-Y.R., Z. Z., Network coding theory, Network Coding Theory, Foundations and Trends in Communication and Information Theory 2 (4 and 5) (2006) 241–381.
14. D. Traskov, M. Heindlmaier, M. Medard, R. Koetter, Scheduling for network-coded multicast, Networking, IEEE/ACM Transactions on 20 (5) (2012) 1479 –1488. doi:10.1109/TNET.2011.2180736.
15. B. Li, Y. Wu, Network coding [scanning the issue], Proceedings of the IEEE 99 (3) (2011) 363 –365. doi:10.1109/JPROC.2010.2096251.
16. S.-Y. Li, Q. Sun, Z. Shao, Linear network coding: Theory and algorithms, Proceedings of the IEEE 99 (3) (2011) 372 –387. doi:10.1109/JPROC.2010.2093851.
17. R. Koetter, M. Medard, An algebraic approach to network coding, IEEE/ACM Transactions on Networking 11 (5) (2003) 782 – 795. doi:10.1109/TNET.2003.818197.
18. T. Ho, M. Medard, R. Koetter, D. Karger, M. Effros, J. Shi, B. Leong, A random linear network coding approach to multicast, IEEE Transactions on Information Theory 52 (10) (2006) 4413 –4430. doi:10.1109/TIT.2006.881746.
19. M. Jafari, L. Keller, C. Fragouli, K. Argyraki, Compressed network coding vectors, in: 2009 IEEE International Symposium on Information Theory (ISIT 2009), 2009, pp. 109 –113. doi:10.1109/ISIT.2010.5513457.
20. J. L. Rebelatto, B. F. Uchôa-Filho, Y. Li, B. Vucetic, Generalized distributed network coding based on nonbinary linear block codes for multi-user cooperative communications, in: 2010 IEEE International Symposium on Information Theory (ISIT 2010), 2010, pp. 943 –947. doi:10.1109/ISIT.2010.5513457.
21. M. Xiao, M. Skoglund, M-user cooperative wireless communications based on nonbinary network codes, in: IEEE Information Theory Workshop on Networking and Information Theory, 2009. (ITW 2009), 2009, pp. 316 –320. doi:10.1109/ITWNIT.2009.5158594.
22. J. Rebelatto, B. Uchoa-Filho, Y. Li, B. Vucetic, Multiuser cooperative diversity through network coding based on classical coding theory, IEEE Transactions on Signal Processing 60 (2) (2012) 916–926. doi:10.1109/TSP.2011.2174787.
23. H. V. Nguyen, C. Xu, S. X. Ng, L. Hanzo, Non-coherent near-capacity network coding for cooperative multi-user communications, IEEE Transactions on Communications 60 (10) (2012) 3059–3070. doi:10.1109/TCOMM.2012.071912.110540.
24. H. V. Nguyen, S. X. Ng, L. Hanzo, Irregular convolution and unity-rate coded network-coding for cooperative multi-user communications, IEEE Transactions on Wireless Communications 12 (3) (2013) 1231–1243. doi:10.1109/TWC.2012.123112.120587.
25. S. X. Ng, J. Wang, L. Hanzo, Unveiling Near-Capacity Code Design: The Realization of Shannon's Communication Theory for MIMO Channels, in: Proc. IEEE International Conference on Communications ICC '08, 2008, pp. 1415–1419. doi:10.1109/ICC.2008.274.
26. A. Ashikhmin, G. Kramer, S. ten Brink, Extrinsic information transfer functions: model and erasure channel properties, IEEE Transactions on Information Theory 50 (11) (2004) 2657–2673. doi:10.1109/TIT.2004.836693.
27. S. ten Brink, Rate one-half code for approaching the Shannon limit by 0.1 dB, Electronics Letters 36 (15) (2000) 1293–1294. doi:10.1049/el:20000953.
28. D. Tse, P. Viswanath, Fundamentals of Wireless Communications, Cambridge: Cambridge University Press, Englewood Cliffs, NJ, USA, 2005.
29. SAGE, Open source mathematics software, in: online source available at http://wwwsagemath.org/.
30. H. Ochiai, P. Mitran, V. Tarokh, Design and analysis of collaborative diversity protocols for wireless sensor networks, in: Proc. VTC2004-Fall Vehicular Technology Conference 2004 IEEE 60th, Vol. 7, 2004, pp. 4645–4649. doi:10.1109/VETECF.2004.1404971.
31. L. Kong, S. X. Ng, R. Maunder, L. Hanzo, Maximum-throughput irregular distributed space-time code for near-capacity cooperative communications, IEEE Transactions on Vehicular Technology 59 (3) (2010) 1511–1517. doi:10.1109/TVT.2010.2040398.
32. A. Tobagi Fouad, M. M. Hira, Joint optimization of physical layer parameters and routing in wireless mesh networks, in: The 9th IFIP Annual Mediterranean, Ad Hoc Networking Workshop (Med-Hoc-Net), 2010 , 2010, pp. 1 –8.